

The photocatalytic degradation of atrazine on nanoparticulate TiO₂ films

T.A. McMurray*, P.S.M. Dunlop, J.A. Byrne

Nanotechnology and Advanced Materials Research Institute, University of Ulster at Jordanstown, Newtownabbey, BT37 0QB, Northern Ireland, UK

Received 7 October 2005; received in revised form 11 January 2006; accepted 14 January 2006

Available online 13 February 2006

Abstract

The photocatalytic removal of atrazine from water was investigated using immobilised TiO₂ films in a stirred tank reactor designed to maximise mass transfer. The degradation of atrazine was demonstrated with a number of breakdown products identified including the stable end product cyanuric acid. The process was monitored using high performance liquid chromatography (HPLC), total organic carbon analysis (TOC) and liquid chromatography–mass spectrometry (LC–MS). A decrease in the TOC was observed and attributed to the oxidative degradation of atrazine side chains. Intermediates identified included 2-chloro-4-acetamido-6-isopropylamino-1,3,5-triazine, 2-chloro-4-ethylamino-6-(1-methyl-1-ethanol)amino-1,3,5-triazine, 2-chloro-4-ethylamino-6-(2-propanol)amino-1,3,5-triazine, 2-hydroxyatrazine, desethylatrazine, deisopropylatrazine, 2-hydroxydesethyl atrazine and cyanuric acid. Operational parameters such as catalyst loading, oxygen concentration, initial pollutant concentration and UV source were investigated. Atrazine removal followed first order kinetics and the rate was dependent upon catalyst loading up to an optimum loading (above which a decrease in the degradation rate was observed). No difference in the rate was observed when either air and O₂ sparging was used. The rate was directly proportional to initial concentration in the range studied. The use of UVB irradiation did not appear to increase the rate of degradation in comparison with UVA irradiation. However, the maximum apparent quantum yield for the photocatalytic degradation was higher under UVB (0.59%) compared to UVA (0.34%).

© 2006 Elsevier B.V. All rights reserved.

Keywords: Atrazine; Photocatalysis; Titanium dioxide; Water treatment

1. Introduction

Persistent organic pollutants (POPs) have been identified as an increasing problem in our drinking water supplies [1]. Such substances can enter the water supply from various sources and are not effectively removed by conventional water treatment processes [2]. Pesticides have been classed as POPs due to their resistance to natural degradation processes, and hence ability to remain in the environment for long periods of time. By their very nature they are designed to be toxic and kill unwanted organisms. They act by interfering with the biochemical and physiological processes that are common to a wide range of living systems, e.g. parathion used for the control of insects on crops, affects the central nervous system and the liver, whereas atrazine used for the control of broad leaf and grassy weeds, inhibits photosynthesis. Although these compounds are designed to be organism specific they can attack non-target organisms and as a

result, cause serious environmental damage. Atrazine {2-chloro-4-ethyl-amino-6-isopropylamino-1,3,5-triazine} is one of the most common pesticides found in ground water sources and drinking water supplies. In some countries restrictions on its use have been implemented, while in others, bans have even been imposed. Atrazine has been detected above the recommended levels (0.1 ppb or $\mu\text{g dm}^{-3}$) throughout Europe [3–5] and the United States [6,7] and is considered as a priority substance by the EC [8]. It is characterised by its high persistence and lifetime of days up to years in the environment [9,10]. Its persistence is due to the stability of the *s*-triazine ring, which inhibits natural degradation. Atrazine has also been reported to have endocrine disrupting capabilities [11,12].

Semiconductor photocatalysis is a possible alternative/complimentary technology for the treatment and purification of polluted water [13–16]. The process utilises a combination of UV light and a semiconductor catalyst and is capable of degrading chemical pollutants by both oxidative and reductive pathways. Titanium dioxide (TiO₂) is the photocatalyst of choice for water treatment investigations because it is non-soluble under normal pH ranges, it is photoactive, photostable, with *Degussa*

* Corresponding author. Tel.: +44 2890 368942; fax: +44 2890 366863.
E-mail address: ta.mcmurray@ulster.ac.uk (T.A. McMurray).

P25 being widely used as the research standard in the field of photocatalysis.

Photocatalysis has been reported to be effective in the degradation of a wide range of pesticides including the triazine herbicides [17], with TiO₂ being the most widely employed photocatalyst for pesticide destruction in water for research studies [18]. Out of all pesticides reported the triazine herbicides are the only group resistant to total mineralisation. So far techniques such as ozonation and removal by adsorption onto activated carbon have been considered to help eliminate atrazine from the environment [19], however it still remains a threat within the environment.

Many workers have studied the photocatalytic degradation of the triazine herbicides, in particular atrazine [19–23]. Hustert et al. [21] studied the photocatalytic treatment of the triazine herbicides, atrazine, simazine, and cyanazine. They reported that the degradation of the triazines occurred by several steps leading to a final stable product, cyanuric acid, and complete mineralisation of atrazine was not observed. It has been reported by others that full mineralisation of the *s*-triazine herbicides does not occur, with cyanuric acid being produced as the final product of degradation, with prolonged photocatalytic treatment required [23]. However, a recent paper has reported the successful degradation of cyanuric acid by the addition of fluoride ions to a TiO₂ suspension [24].

Photocatalytic degradation under solar irradiation has been reported to be effective for the photocatalytic degradation of *s*-triazines [20,22]. Konstantinou et al. [22] investigated the photocatalytic treatment of *s*-triazine herbicides and organophosphates insecticides using a TiO₂ suspension irradiated under simulated solar light. They reported half-lives ranging from 10.8 to 38.3 min for the *s*-triazines under their reactor conditions, but complete mineralisation again was not observed. Minero et al. [20] investigated the photolytic and photocatalytic degradation of atrazine in a large-scale solar reactor. They reported that atrazine was degraded by photolysis alone (in the absence of photocatalyst), but there was no reduction in the TOC. However, with TiO₂ photocatalyst present, the rate of degradation increased over that observed with photolysis and a reduction in the TOC was observed. However, complete mineralisation to CO₂ was not observed and the reduction in the TOC corresponded to the oxidation of the lateral side chains with only five of the eight carbons of atrazine removed.

Hequet et al. [19] investigated the photolytic and photocatalytic degradation of atrazine and reported efficient UV photolysis with $t_{1/2} < 5$ min and hydroxyatrazine generated as the main intermediate. Cyanuric acid was reported as the final end product. In contrast, under photocatalysis, atrazine was found to have a $t_{1/2} \sim 20$ min, with desalkylated compounds as the major intermediates, with final degradation to cyanuric acid. Therefore the photocatalytic degradation followed the pathway involving oxidation of the lateral side chains rather than the hydroxylation pathway as seen with photolysis. The half-lives reported for the photolysis and photocatalysts cannot be directly compared, as the wavelengths and intensity of the radiation differ in both cases. The majority of research carried out has involved suspensions of TiO₂ though a few studies have been conducted on immo-

Table 1

Compound names and abbreviation for atrazine and intermediate photodegradation products

Abbreviation	Compound
Atrazine	2-Chloro-4-ethylamino-6-isopropylamino-1,3,5-triazine
AOHE	2-Chloro-4-acetamido-6-isopropylamino-1,3,5-triazine
AOHI1	2-Chloro-4-ethylamino-6-(1-methyl-1-ethanol)amino-1,3,5-triazine
AOHI2	2-Chloro-4-ethylamino-6-(2-propanol)amino-1,3,5-triazine
OHA	2-Hydroxyatrazine
DEA	Desethylatrazine
DIA	Deisopropylatrazine
DAA	Desethyldeisopropyl atrazine
OHDEA	2-Hydroxydesethyl atrazine
OHDA	2-Hydroxydesisopropyl atrazine
Cl(OH)NH ₂	2-Chloro-4-amino-6-hydroxy-1,3,5-triazine
Cl(OH) ₂	2-Chloro-4-hydroxy-6-hydroxy-1,3,5-triazine
OHOHIDEA	2-Hydroxy-4-amino-6-(1-methyl-1-ethanol)amino-1,3,5-triazine
OHOEDIA	2-Hydroxy-4-acetamido-6-amino-1,3,5-triazine
AME	2-Hydroxy-4,6-diamino-1,3,5-triazine
ADE	2,4-Dihydroxy-6-amino-1,3,5-triazine
CYA	2,4,6-Trihydroxy-1,3,5-triazine

bilised films [25–30]. A list of identified intermediates and their abbreviations reported in literature for the photodegradation of atrazine are given in Table 1.

The photocatalyst may be used either in the slurry or immobilised form. Using an immobilised system one can obtain a configuration in which all the catalyst is illuminated and further eliminates the need for post treatment catalyst recovery. A disadvantage with an immobilised system is that mass transfer limitations can reduce reactor efficiency and/or interfere with the measurement of true degradation kinetics. This paper reports on the photocatalytic degradation of atrazine on immobilised TiO₂ films in a stirred tank reactor which has been specifically designed to maximise mixing and mass transfer and thus give more accurate measurement of intrinsic degradation kinetics.

2. Materials and methods

2.1. Immobilisation of TiO₂

TiO₂ (Degussa P25) was immobilised onto indium doped tin oxide coated borosilicate glass (Donnelley Co-Operation USA) using an electrophoretic deposition technique [31] by applying a fixed negative potential of 25 V to the conducting glass for a set period of time. The TiO₂-ITO glass was then annealed in air at 673 K for 1 h to effect particle adhesion and cohesion. Gravimetric analysis was used to determine the TiO₂ loading.

2.2. Photocatalytic reactor

A custom built stirred tank photo-reactor (STR) previously reported [32], was used to study the photocatalytic degradation of atrazine in water. The system consisted of a water-jacketed walled vessel creating a reservoir and a stainless steel propeller used to create a turbulent flow within. Good mass transfer

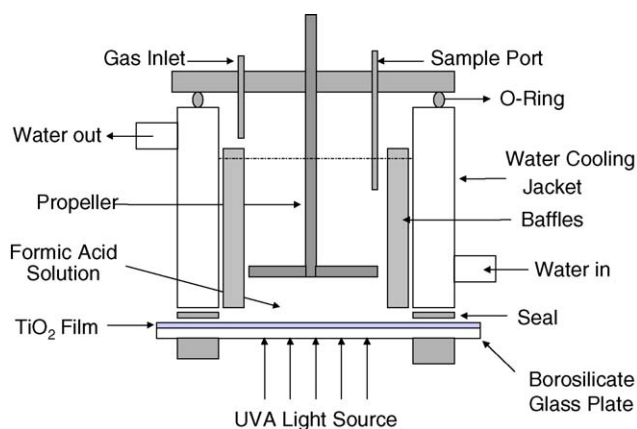


Fig. 1. Schematic representation of a stirred tank reactor.

behaviour is obtained as turbulent flow within the reactor transports the organic pollutant towards the coated TiO₂ plate and disperses O₂ from the headspace into the liquid. The coated TiO₂-ITO glass plate was illuminated from below using either two UV-A fluorescent lamps (Philips, PL-S 9W/10, peak emission 370 nm) or two UV-B fluorescent lamps (Philips, PL-S 9W/12, peak emission 310 nm) positioned at a distance of 2.5 cm away from the TiO₂ glass plate. The light intensity entering the reactor was determined by potassium ferrioxalate actinometry [33]. Oxygen (99.5%) or air was added to the headspace of the reactor at a constant flow of 900 cm³ min⁻¹. A schematic representation of the STR is given in Fig. 1. Operational parameters of the reactor have been previously studied for the degradation of formic acid [32].

2.3. Photocatalytic experiments

In a typical experiment the UV lamps were switched on and allowed to stabilise for 20 min. An aqueous solution (200 cm³) of atrazine (Riedel-de-Haen) with the desired concentration (normally 9.3×10^{-5} mol dm⁻³/20 ppm), was added to the reactor and equilibrated for 15 min in the dark with gas sparging. The propeller was switched on and adjusted to the required speed (2000 rpm). A 1.5 cm³ sample was taken ($t=0$ s), the UV screen was removed, and further samples were taken every 15 min thereafter, usually for 3 h.

2.4. Analytical methods

2.4.1. High performance liquid chromatography (HPLC)

Atrazine concentration was determined using reverse phase HPLC (Supelco Discovery C18 column 150 mm × 4.6 mm i.d., 5 μm). Separation was by isocratic elution with mobile phase 33 MeCN: 66 H₂O at a flow rate of 1.0 cm³ min⁻¹. 20 μl was injected on column with the column temperature maintained at 20 °C. Detection was by UV absorption at $\lambda = 214$ nm. The presence of cyanuric acid was identified using reverse phase HPLC (ODS Phenomenex Bondclone 10 column hyper-sil length 300 mm; i.d. 3.9 mm; particle size 10 μm) with 95, 5×10^{-4} M Na₂HPO₄:5 MeOH mobile phase at a flow rate of 0.5 cm³ min⁻¹. 20 μl was injected on column with the column

temperature maintained at 35 °C. Detection was at $\lambda = 213$ nm. Quantitative analysis was not possible with the above column due to coelution with other intermediates. The instrumentation consisted of a Spectra Physics P2000 pump, Thermoseparation AS1000 autosampler, Spectra Physics LIS UV/Vis detector and Thermoquest PC1000 software.

Two separate columns were used for the detection of atrazine and cyanuric acid due to cyanuric acid not being detectable using the Supelco C18 column (recommended for the detection of triazine herbicides) as it was found to co-elute alongside the solvent front. By using the ODS Phenomenex Bondclone 10 column better separation characteristics were obtained for the detection of cyanuric acid. However atrazine could not be detected on this column due to co-elution with other intermediate products. Therefore the two systems were used independently of each other. The intermediate products produced during the degradation of atrazine to cyanuric acid could not be detected with the Supelco C18 column and poor separation was achieved using the ODS Phenomenex column due to co-elution. LC-MS was used to identify the presence of these intermediate products.

2.4.2. Liquid chromatography-mass spectrometry (LC-MS)

A LCQ quadrupole ion-trap mass spectrometer (Finnigan MAT, San Jose, CA, USA) utilising electrospray ionisation (ESI) was used for the determination of intermediate products formed during the photocatalytic degradation of atrazine. The samples for MS characterisation were infused into the mass spectrometer at a flow rate of 0.5 cm³ min⁻¹. In the ESI source nitrogen sheath and auxiliary gas flows were maintained at 50 and 5 units, respectively. The heated capillary temperature was 220 °C and the spray voltage set to 4.5 kV. The chromatographic conditions were the same as those described for atrazine detection.

2.4.3. Total organic carbon analysis (TOC)

TOC analysis was carried out using a Shimadzu 5000A TOC analyser. This system uses a Pt furnace at 650 °C with detection of carbon by IR-CO₂ analysis. Inorganic carbon (IC) is measured by CO₂ analysis following acidification. Total carbon (TC) – IC = TOC.

3. Results and discussion

Atrazine was photocatalytically degraded under UVA irradiation using immobilised TiO₂ films. A rapid initial decrease in the pesticide concentration ($t_{1/2} < 24.5$ min) was observed with irradiation time between 0 and 100 min with complete disappearance after ~150 min. The degradation followed pseudo first order kinetics where a semi-log plot of concentration versus time gave a straight line. Similar kinetics have been reported by other workers [22,25,34,35].

For comparison of data, initial rates have been to compare the photocatalytic degradation of atrazine under different conditions and parameters and were calculated using the following equation:

$$\text{Rate}_{\text{int}} = k_{\text{obs}}[S] \quad (1)$$

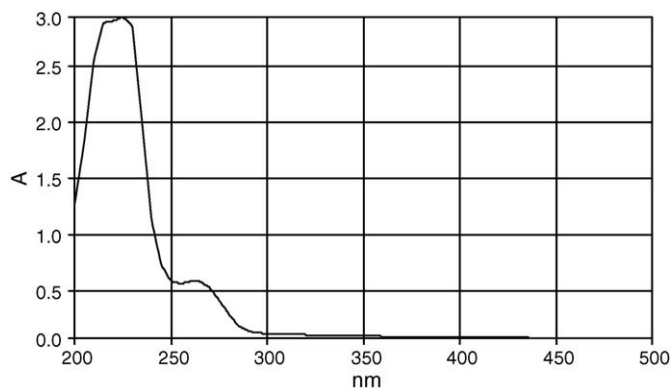


Fig. 2. Absorption spectrum of atrazine over 200–500 nm.

Where the pseudo first order rate constant k_{obs} was determined from a semi-log plot of concentration versus time.

No degradation of the parent atrazine was observed in the absence of TiO_2 or UV irradiation. Photolytic degradation of atrazine was not expected in our system since the absorption spectrum of atrazine shows only UV absorbance below 270 nm (Fig. 2) and the lamps used in this study emit light at $\lambda > 300$ nm.

The TOC decreased from an initial 10.6 ppm (4.95×10^{-5} mol dm^{-3} atrazine) to 6.3 ppm (2.92×10^{-5} mol dm^{-3}) after 300 min photocatalysis (Fig. 3). This incomplete decrease in TOC (40%) can be attributed to partial removal of the carbon within the atrazine side chains. For complete degradation of atrazine to cyanuric acid, a decrease in TOC of $\sim 60\%$ would be expected, corresponding to complete oxidation of the lateral side chains with the number of carbons being reduced from eight to three. A 40% decrease would suggest that the number of carbons were reduced from eight to five. C5 compounds in the degradation pathway of atrazine include deisopropylatrazine (DIA), 2-hydroxydeisopropyl atrazine (OHDIA) and 2-hydroxy-4-acetamido-6-amino-1,3,5-triazine (OHOEDIA). Further intermediates in the degradation pathway may be present but were not detectable. The complete disappearance of atrazine occurs at around 150 min, whereas under the same working

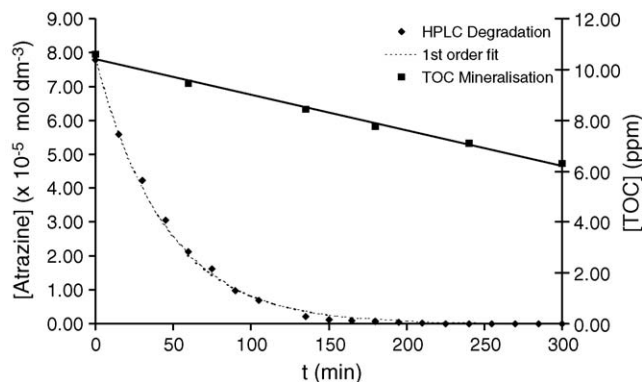


Fig. 3. Corresponding rate of atrazine mineralisation with degradation of atrazine.

conditions the corresponding TOC is still decreasing at around 300 min.

Fig. 4 shows an HPLC trace illustrating the disappearance of atrazine over time. The atrazine peak is removed below detectable limits with the formation of a number of intermediates. The peaks due to intermediates formed subsequently decrease, with the appearance of other peaks due to the formation of other intermediates. Finally a large peak is formed at RT 2 min after 180 min of photocatalytic treatment. This peak was in part due to cyanuric acid, confirmed by LC-MS.

3.1. Identification of intermediates produced during degradation

Atrazine was subjected to photocatalytic treatment for 22 h with samples taken every 30 min for the first 7 h, and a further sample taken at 9 and 22 h. Atrazine was degraded below detectable limits within the first 180 min of photocatalytic treatment. However, complete conversion to cyanuric acid cannot be confirmed over that time period.

HPLC analysis demonstrated that a number of intermediate compounds were formed as the concentration of the parent

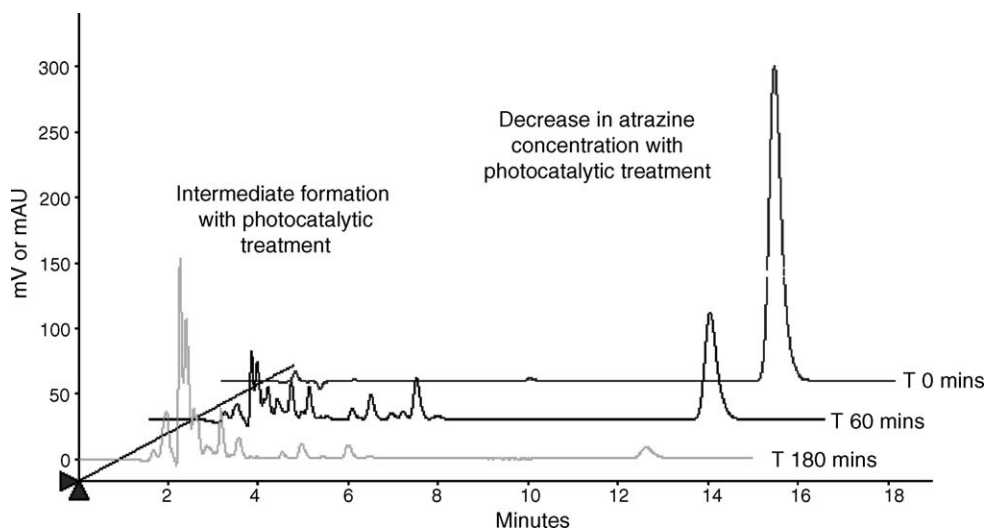


Fig. 4. HPLC spectrum for time 0, 60 and 180 min of photocatalytic treatment, showing decrease of atrazine and the increasing formation of intermediates.

Table 2
Identified intermediates by LCMS with their corresponding m/z values

Identified compound	Mass spectrum (m/z) ^a
Atrazine	216.1
AOHI1/AOHI2	232.2
AOHE	230.0
OHA	198.2
DEA	188.1
DIA	174.1
OHDEA	170.1
Cyanuric acid	129.07

^a MS analysis in +ve ion mode.

atrazine decreased. Comparing retention times with standards of reported intermediates allowed their identification of the intermediates being formed. When the samples were analysed by LC–MS the intermediates responsible for the peaks could be identified. A list of the identified intermediates are listed in Table 2 and it was found that they were in accordance with the pathway previously proposed by Hequet et al. [19]. The primary pathway for atrazine degradation on nanoparticulate TiO₂ films involved the oxidation of the lateral side chains of atrazine, producing the dealkylated derivatives, 2-chloro-4-acetamido-6-isopropylamino-1,3,5-triazine (AOHE), 2-chloro-4-ethylamino-6-(2-propanol)amino-1,3,5-triazine (AOHI1), 2-chloro-4-ethylamino-6-(2-propanol)amino-1,3,5-triazine (AOHI2), desethylatrazine (DEA), deisopropylatrazine (DIA) and desethyldeisopropyl atrazine (DAA). Hydrolysis of the chlorine substituent in desethylatrazine (DEA), desethyldeisopropyl atrazine (DAA) and deisopropylatrazine (DIA) leads to production of 2-hydroxydesethyl atrazine (OHDEA) with the further displacement of the amino groups by hydroxyl groups resulting in cyanuric acid. The secondary pathway follows a hydroxylated pathway with immediate substitution of the chlorine at position two with a hydroxyl group.

3.2. Effect of catalyst loading

TiO₂ loadings ranging from 1.60 to 0.19 mg cm⁻² were prepared and the optimum catalyst loading determined for the degradation of atrazine. The initial rate increased with TiO₂ loading up to an optimum of ~1.10 mg cm⁻² (Fig. 5). Loadings greater than this optimum resulted in a decrease in the rate of degradation. A similar trend was observed by Hasegawa et al. [36] with aqueous suspension of TiO₂ for photocatalytic degradation of iprobenfos. The rate increased up to an optimum loading, then decreased slightly until a constant was obtained. An optimum TiO₂ loading of 0.5 mg cm⁻³ was found for the degradation of iprobenfos, with a similar dependence also observed

Table 3
Initial rates of atrazine degradation at differing O₂ concentrations

Electron acceptor	% O ₂ composition	Rate _{int} ($\times 10^{-10}$ mol cm ⁻² s ⁻¹)	S.D. of values ($\times 10^{-12}$)
Oxygen	100	1.13	2.15
Air	20	1.11	0.85
Oxygen free nitrogen	0	0.02	0.75

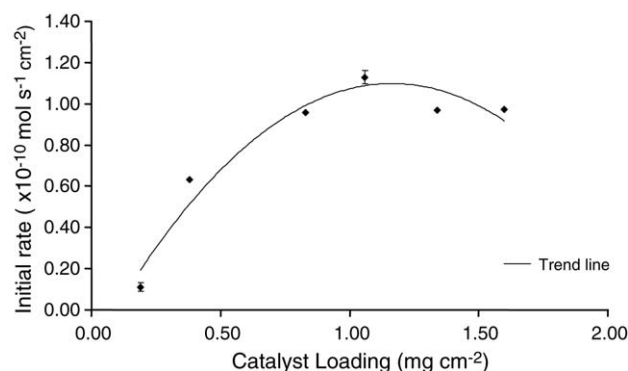


Fig. 5. Initial Rate of atrazine degradation as a function of catalyst loading.

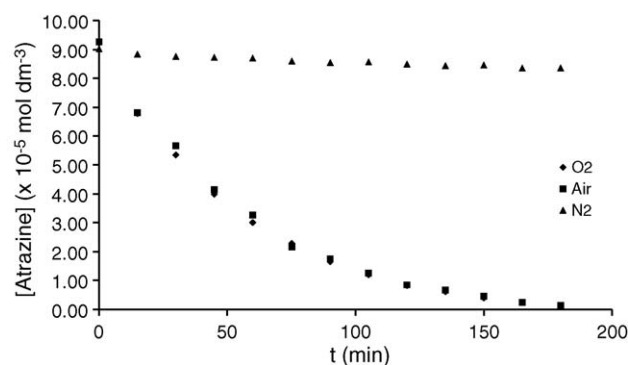


Fig. 6. Disappearance of atrazine over time in the presence of O₂, air and OFN.

for nine other agrochemicals including the *s*-triazine simazine. It is difficult to draw comparisons to optimum values for catalyst loadings between research workers, as the dependence of rate on the TiO₂ loading will vary for different reactors and irradiation sources etc, however general trends can be noted. The trend can be explained by the fact that as the catalyst film becomes too thick the TiO₂ will begin to effectively mask itself with the total irradiation being absorbed by only the initial layers of the catalyst. The maximum rate, under the conditions of these experiments, will be achieved when all of the incident light is absorbed by the catalyst film. This occurs, for I_0 ($\lambda = 370$ nm) = 3.28×10^{-8} Einstein cm⁻² s⁻¹ when the catalyst loading is approximately 1.10 mg cm⁻² (Fig. 5).

3.3. Effect of oxygen concentration

The effect of O₂ concentration was investigated for the initial degradation of atrazine using O₂ (100%), air (20% O₂) and OFN (oxygen free nitrogen). Fig. 6 shows the disappearance of atrazine over time for O₂, air and OFN and the initial rates are given in Table 3. Under OFN sparging the rate of degrada-

tion was only 2% of that observed under air sparged conditions. Under O₂ sparging there was only a 2% increase in the degradation rate compared to air sparging. The initial concentration of atrazine in these experiments was in the micromolar range ($9.3 \times 10^{-5} \text{ mol dm}^{-3}$). Previously the photocatalytic degradation of formic acid (initial concentrations in the millimolar range) was analysed in this reactor [37] and it was found that there was only a small increase in the rate of degradation with increasing O₂ concentration above air saturation (20%). Therefore, it is unlikely that the reduction of O₂ would be the rate limiting for the degradation of atrazine at 20% O₂ or above. Gerischer and Heller [38] reported the removal of conduction band electrons may be rate limiting at high pollutant concentrations/or low oxygen concentrations in photocatalytic destruction of pollutants.

3.4. Effect of initial pollutant concentration

Pesticides are found at extremely low levels in water, i.e. ppb levels with the maximum limit allowed by the European Directive for single pesticides being $0.1 \mu\text{g dm}^{-3}$ (for atrazine

equivalent to $4.64 \times 10^{-10} \text{ mol dm}^{-3}$ [39]). To study the photocatalytic degradation at such low levels requires extremely sensitive analytical methods. The HPLC method for atrazine detection is not capable of detecting atrazine at such low levels without pre-concentration and therefore, a concentration of $9.27 \times 10^{-5} \text{ mol dm}^{-3}$ atrazine was used in experiments and the limit of detection by HPLC was $2.59 \times 10^{-8} \text{ mol dm}^{-3}$.

Experiments were performed at $1.39 \times 10^{-4} \text{ mol dm}^{-3}$ (30 ppm), $1.15 \times 10^{-4} \text{ mol dm}^{-3}$ (25 ppm), $9.27 \times 10^{-5} \text{ mol dm}^{-3}$ (20 ppm), $6.95 \times 10^{-5} \text{ mol dm}^{-3}$ (15 ppm), $4.64 \times 10^{-5} \text{ mol dm}^{-3}$ (10 ppm), $2.32 \times 10^{-5} \text{ mol dm}^{-3}$ (5 ppm) concentrations of atrazine. Plots of $\ln[S]_t/[S]_0$ versus time for each concentration (Fig. 7) suggested that the kinetics appeared to deviate from first order kinetics at lower concentrations, and therefore a trend line was taken over the linear region of the plot and the initial rates calculated (Table 4). If the kinetics obey true first order, k_{obs} remains constant over a range of $[S]_0$. As the concentration of atrazine was increased, k_{obs} decreased slightly. Initial rate increased proportionally with initial concentration in the range studied (Fig. 8). A double reciprocal plot of the data also yielded a good fit to a straight line. However the data range is

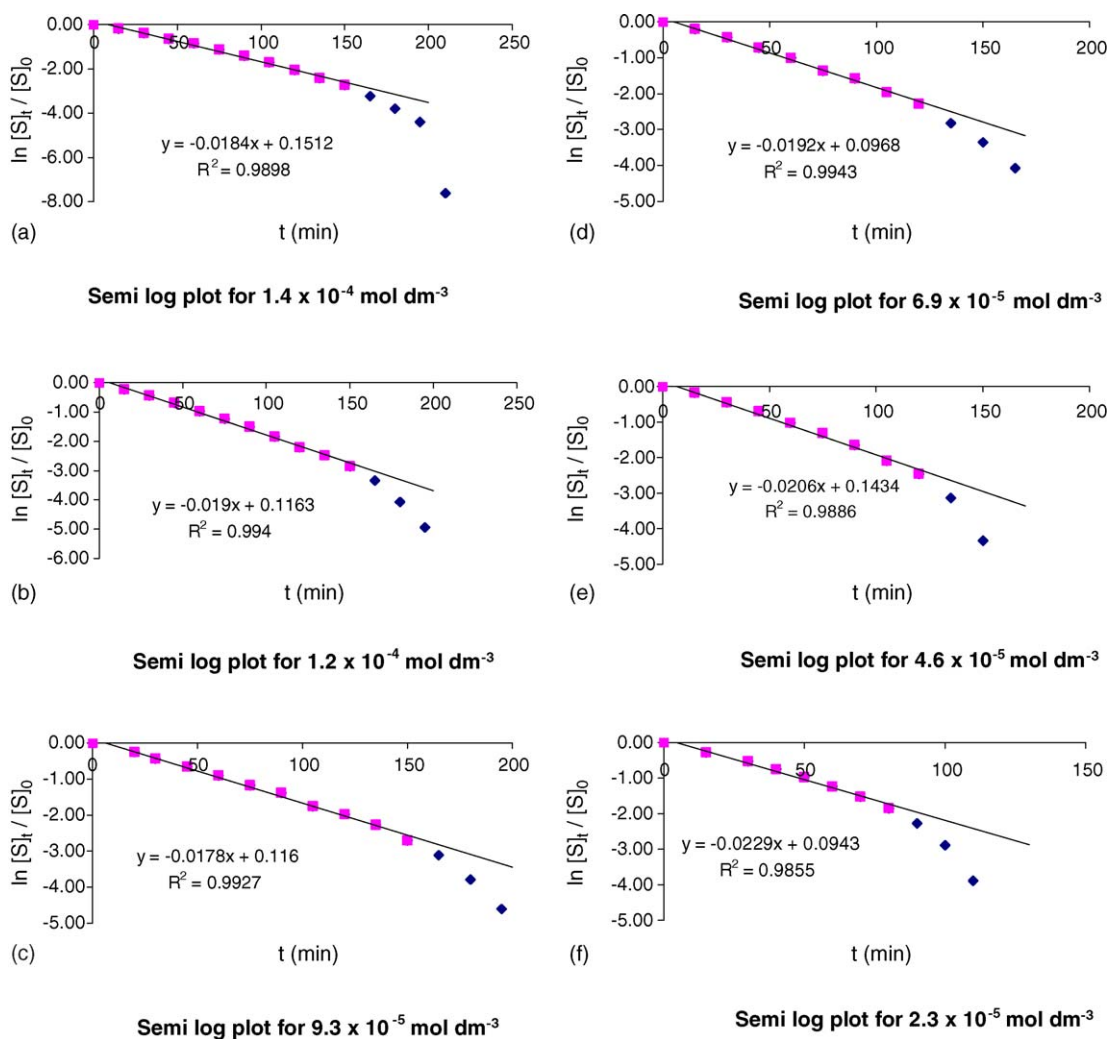


Fig. 7. Semi-log plots of $\ln[S]_t/[S]_0$ over time were plotted for each initial concentration of atrazine studied.

Table 4

Calculated pseudo first order rate constants, initial rates with corresponding number of data points used and R^2 values for effect of initial concentration of atrazine on initial degradation rate

$[S]_0$ ($\times 10^{-4}$ mol dm $^{-3}$)	k_{obs} (min $^{-1}$)	Rate $_{\text{int}}$ ($\times 10^{-10}$ mol dm $^{-3}$ cm $^{-2}$)	R^2	Data points
1.39	0.0184	1.50	0.9898	11
1.16	0.0190	1.29	0.9940	11
0.93	0.0178	0.97	0.9927	11
0.69	0.0192	0.78	0.9943	9
0.46	0.0206	0.56	0.9886	9
0.23	0.0229	0.31	0.9855	8

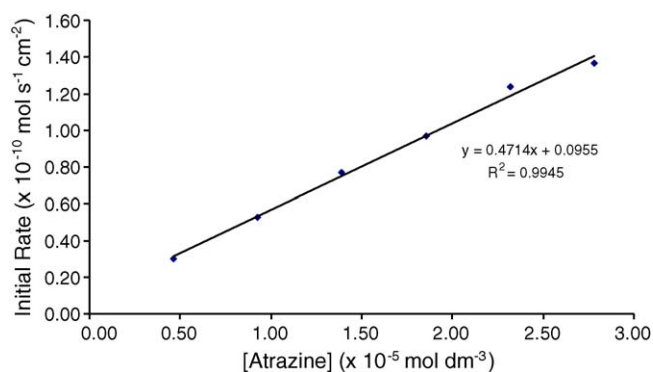


Fig. 8. Initial rate of atrazine degradation as a function of initial concentration.

limited and it is not possible to say if photocatalytic degradation of atrazine follows a Langmuir–Hinshelwood type kinetic model, often used to describe the degradation of pollutants [14,40,41].

3.5. Comparison of UVA and UVB irradiation

Experiments were carried out using UVB irradiation in order to determine if light of higher energy would enhance the rate of photocatalytic degradation. Experiments were carried out in O₂, air and OFN sparged conditions under UVB irradiation. The calculated initial rates given in Table 5. The results for O₂, air and OFN sparging under UVA irradiation are given for comparison. For O₂ and air sparging no marked difference was observed for the initial degradation rate using UVB irradiation.

When comparing the initial degradation rates for UVA and UVB the rate of degradation under O₂ sparged conditions were very similar. A 5% increase was observed under air sparging with UVB irradiation compared to UVA. Under OFN sparging an increase of 50% was observed, though the rate of degradation was not comparable with that obtained under air or O₂ sparging.

No marked difference in the rate of degradation of atrazine under light of higher energy, i.e. UVB, $\lambda_{\text{max}} = 313$ nm in comparison with UVA irradiation, $\lambda_{\text{max}} = 365$ nm.

In previous studies involving the photocatalytic degradation of formic acid in this system [37], higher rates were obtained under UVB irradiation than with UVA (20 and 17% increase with O₂ and air sparging, respectively), though the concentration of formic acid was of a higher order than that of atrazine in this study. Stafford et al. and Blazkova et al. suggested that the increase in degradation was due to the light of higher energy promoting the electrons into a higher energy level in the conduction band thus reducing the likelihood of recombination with the photogenerated holes, than those electrons that are promoted to the lowest unoccupied molecular orbital [42,43]. Also the absorption coefficient (ϵ) of TiO₂ increases with decreasing wavelength with maximum absorption at $\lambda = 250$ nm [44]. The low concentration of atrazine present could be a rate limiting factor, thus why no increase in the rate of degradation was observed under UVB irradiation.

The apparent quantum yield (Φ_{app}) for atrazine degradation can be calculated by dividing the initial rate by the incident photon flux (I_0) [15]. The light intensity falling upon the reactor was determined by potassium ferrioxalate actinometry [33]. For UVA irradiation the $I_0 = 3.28 \times 10^{-8}$ Einstein cm $^{-2}$ s $^{-1}$ and for UVB irradiation, $I_0 = 2.0 \times 10^{-8}$ Einstein cm $^{-2}$ s $^{-1}$. Φ_{app} was calculated for experiments carried out under O₂ and air sparging for both UVA and UVB irradiation (Table 5). The highest Φ_{app} values were obtained for UVB irradiation. This was in agreement with results previously obtained for formic acid degradation [37]. However, it should be noted that Φ_{app} obtained for the photocatalytic degradation of atrazine under UVB irradiation were significantly lower than those obtained with formic acid, however the concentration used for atrazine degradation (9.3×10^{-5} mol dm $^{-3}$) was much lower in comparison to that used for formic acid degradation

Table 5

Calculated initial rates of degradation and quantum yields under UVA/B irradiation and O₂, air and OFN sparging

Conditions	UVA		UVB	
	Rate ($\times 10^{-10}$ mol cm $^{-2}$ s $^{-1}$)	Φ_{app} (%)	Rate ($\times 10^{-10}$ mol cm $^{-2}$ s $^{-1}$)	Φ_{app} (%)
O ₂	1.13	0.34	1.12	0.56
Air	1.11	0.34	1.17	0.59
OFN	0.02	0.01	0.03	0.02

3.6. Control experiments

Control experiments were carried out in the absence of TiO₂, light and O₂. No significant atrazine degradation was observed unless TiO₂, light and O₂ were present. All control experiments were monitored for a period of 180 min, which was, long enough for the complete removal of the parent atrazine under photocatalytic conditions with O₂ present. No photolysis of atrazine was observed either with the UVA or UVB source.

4. Conclusion

The photocatalytic degradation of the pesticide, atrazine and the formation of intermediates were followed using HPLC, TOC, and LC–MS. The parent compound, atrazine, was completely degraded, as confirmed by HPLC. However, the removal of TOC was much slower than the degradation of the parent compound and complete TOC removal was not observed. This was attributed to the removal of the carbon within the atrazine side chains. The TOC value decreased by approximately 40%, which suggested a reduction from eight carbons to five, suggesting the presence of DIA, OHDIA and OHOEDIA. A stable end product, cyanuric acid, was also found to be present and this finding is consistent with other researchers. The degradation pathway was investigated using LC–MS. The identified intermediates were consistent with that reported by others.

A range of TiO₂ loadings were examined, with the optimum catalyst loading determined to be 1.1 mg cm⁻³. The effect of oxygen concentration was also examined with no difference observed between air and O₂ sparging. It is thought that this is due to the efficiency of the STR and the mixing that occurs within, and that above oxygen concentrations of >20% the reduction of oxygen would be less likely to be the rate limiting factor. As initial atrazine concentration was increased the rate increase proportionally however it was not possible to fit the data to a Langmuir–Hinshelwood type kinetic model due to the limited concentration range studied.

The use of UVB irradiation did not markedly increase the rate of degradation in comparison with UVA irradiation, though the apparent quantum yields obtained with UVB were slightly higher than those obtained with UVA. While complete mineralisation of atrazine was not observed it remains that the parent compound, which is both toxic and has suspected endocrine disrupting properties, was degraded to a less problematic compound, cyanuric acid. Photocatalysis is therefore a possible treatment for water sources contaminated with atrazine.

Acknowledgements

The authors would like to thank Degussa (Germany) for supplying samples of P25, Philips lighting (Netherlands) for supplying UV lamps, the engineering technical staff of the University of Ulster for reactor construction, the Chemical Engineering Department of the University of Groningen (Netherlands) for the design of the reactor and Dr. Stephen McClean and Mr. Eddie O’Kane at University of Ulster, Coleraine for help and use of LC–MS. Also, the European commission for funding

PCATIE (ENV4-CT97-0632) and PEBCAT (EVK1-CT-2000-00069) and the Department of Education and Learning, Northern Ireland, for funding T.A. McMurray.

References

- [1] N. Gray, *Drinking Water Quality. Problems and Solutions*, John Wiley & Sons, 1994, pp. 132–148.
- [2] I.R. Bellobono, F. Gianturco, C.M. Chiodaroli, *Fresenius Environ. Bull.* 6 (1997) 469–474.
- [3] D.P. Hessler, V. Gorenflo, F.H. Frimmel, *Acta Hydrochim. Hydrobiol.* 21 (1993) 209–214.
- [4] M.F. Legrand, E. Costentin, A. Bruchet, *Environ. Technol.* 12 (1991) 985–996.
- [5] S.R. Muller, M. Berg, M.M. Ulrich, R.P. Schwarzenbach, *Environ. Sci. Technol.* 31 (1997) 2104–2113.
- [6] D.W. Kolpin, S.J. Kalkhoff, *Environ. Sci. Technol.* 27 (1993) 134–139.
- [7] W.E. Pereira, C.E. Rostad, *Environ. Sci. Technol.* 24 (1990) 1400–1406.
- [8] Decision no 2455/2001/EC of the European Parliament and of the Council of 20 November 2001 establishing the list of priority substances in the field of Water Policy and Amending Directive 2000/60/E, L331/1 (2001).
- [9] S. Comber, M. Gardner, *Sci. Total Environ.* 244 (1999) 193–201.
- [10] D.A. Goolsby, E.M. Thurman, M.L. Pomes, M.T. Meyer, W.A. Battaglin, *Environ. Sci. Technol.* 31 (1997) 1325–1333.
- [11] Pesticide Action Network UK, Briefing Paper—Pesticides in water: costs to health and the environment. <http://www.pan-uk.org/briefing/water.pdf>, October 2000 (accessed January 2005).
- [12] T. Hayes, K. Haston, M. Tsui, A. Hoang, C. Haeffele, A. Vonk, *Environ. Health Perspect.* 111 (2003) 568–575.
- [13] P.R. Gogate, A.B. Pandit, *Adv. Environ. Res.* 8 (2004) 501–551.
- [14] M.R. Hoffmann, S.T. Martin, W.Y. Choi, D.W. Bahnemann, *Chem. Rev.* 95 (1995) 69–96.
- [15] A. Mills, S. LeHunte, *J. Photochem. Photobiol. A-Chem.* 108 (1997) 1–35.
- [16] I.K. Konstantinou, T.A. Albanis, *Appl. Catal. B-Environ.* 42 (2003) 319–335.
- [17] H.D. Burrows, M. Canle, J.A. Santaballa, S. Steenzen, *J. Photochem. Photobiol. B-Biol.* 67 (2002) 71–108.
- [18] S. Chiron, A. Fernandez-Alba, A. Rodriguez, E. Garcia-Calvo, *Water Res.* 34 (2000) 366–377.
- [19] V. Hequet, C. Gonzalez, P. Le Cloirec, *Water Res.* 35 (2001) 4253–4260.
- [20] C. Minero, E. Pelizzetti, S. Malato, J. Blanco, *Sol. Energy* 56 (1996) 411–419.
- [21] K. Hustert, P.N. Moza, B. Pouyet, *Toxicol. Environ. Chem.* 31-2 (1991) 97–102.
- [22] I.K. Konstantinou, T.M. Sakellarides, V.A. Sakkas, T.A. Albanis, *Environ. Sci. Technol.* 35 (2001) 398–405.
- [23] E. Pelizzetti, V. Maurino, C. Minero, V. Carlin, E. Pramauro, O. Zerbini, M.L. Tosato, *Environ. Sci. Technol.* 24 (1990) 1559–1565.
- [24] Y.C. Oh, W.S. Jenks, *J. Photochem. Photobiol. A-Chem.* 162 (2004) 323–328.
- [25] G. Chester, M. Anderson, H. Read, S. Esplugas, *J. Photochem. Photobiol. A-Chem.* 71 (1993) 291–297.
- [26] F. Gianturco, C.M. Chiodaroli, I.R. Bellobono, M.L. Raimondi, A. Moroni, B. Gawlik, *Fresenius Environ. Bull.* 6 (1997) 461–468.
- [27] S. Parra, S. Malato, C. Pulgarin, *Appl. Catal. B-Environ.* 36 (2002) 131–144.
- [28] S. Parra, S.E. Stanca, I. Guasaquillo, K.R. Thampi, *Appl. Catal. B-Environ.* 51 (2004) 107–116.
- [29] K. Macounova, J. Urban, J. Krysa, J. Jirkovsky, J. Ludvik, *J. Photochem. Photobiol. A-Chem.* 140 (2001) 93–98.
- [30] J.C. Lee, M.S. Kim, B.W. Kim, *Water Res.* 36 (2002) 1776–1782.
- [31] J.A. Byrne, B.R. Eggins, N.M.D. Brown, B. McKinney, M. Rouse, *Appl. Catal. B-Environ.* 17 (1998) 25–36.
- [32] T.A. McMurray, J.A. Byrne, P.S.M. Dunlop, J.G.M. Winkelmann, B.R. Eggins, E.T. McAdams, *Appl. Catal. A-Gen.* 262 (2004) 105–110.

- [33] J. Calvert, J. Pitts, *Experimental methods in photochemistry*, in: *Photochemistry*, John Wiley and Sons, 1973, pp. 686–798.
- [34] H. Krysova, J. Jirkovsky, J. Krysa, G. Mailhot, M. Bolte, *Appl. Catal. B-Environ.* 40 (2003) 1–12.
- [35] G.A. Penuela, D. Barcelo, *J. AOAC Int.* 83 (2000) 53–60.
- [36] K. Hasegawa, T. Kanbara, S. Kagaya, *Denki Kagaku.* 66 (1998) 625–634.
- [37] T.A. McMurray, J.A. Byrne, P.S.M. Dunlop, E.T. McAdams, *J. Appl. Electrochem.* 35 (2005) 723–731.
- [38] H. Gerischer, A. Heller, *J. Phys. Chem.* 95 (1991) 5261–5267.
- [39] Council Directive 98/83/EEC on the quality of water intended for human consumption, L330 (1998) 32–54.
- [40] C.S. Turchi, D.F. Ollis, *J. Catal.* 122 (1990) 178–192.
- [41] R.W. Matthews, *J. Catal.* 111 (1988) 264–272.
- [42] A. Blazkova, I. Csolleova, V. Brezova, *J. Photochem. Photobiol. A-Chem.* 113 (1998) 251–256.
- [43] U. Stafford, K.A. Gray, P.V. Kamat, *J. Catal.* 167 (1997) 25–32.
- [44] B. Blanckenhagen, D. Tonova, *Characterisation of thin film materials for optical coatings: approaches beyond UV/VIS/NIR spectroscopy*, in: *Abstracts of the Colloquium on Optical Spectrometry*, Berlin, 2002.